CASE STUDY OF DESIGN OPTIMIZATION OF MULTI-CAVITY FILTERS WITH MISMATCHED TERMINATIONS

J.W. Bandler and S.H. Chen

SOS-85-3-R

January 1985

CASE STUDY OF DESIGN OPTIMIZATION OF MULTI-CAVITY FILTERS WITH MISMATCHED TERMINATIONS

J.W. Bandler and S.H. Chen

Abstract

Examples of multi-coupled cavity filters with mismatched terminations are presented. Cases studied include 6th order filters with complex constant and frequency-dependent source impedances as well as a 6th order singly terminated design. All the examples considered are synchronously tuned. Network variables and data related to the optimization process are provided.

This work was supported in part by the Natural Sciences and Engineering Research Council of Canada under Grant G1135.

The authors are with the Simulation Optimization Systems Research Laboratory and the Department of Electrical and Computer Engineering, McMaster University, Hamilton, Canada L8S 4L7.

I. INTRODUCTION

An approach to interactive design optimization of multi-coupled cavity microwave filters has been proposed in [1]. Implementing our approach on a CDC 170/730 digital computer, a computer program has been constructed and successfully tested for various filter design problems. An efficient method of filter simulation and sensitivity evaluation, namely the loaded filter approach, as presented in Section IV of [2], is utilized. Some selected numerical examples have been reported previously in [3] and [4].

The design of filters with mismatched terminations is of great interest in the construction of multiplexing networks. Here, mismatched terminations refer to complex and possibly frequency dependent source impedances, load impedances, a combination of both or singly terminated structures. The case of unequal resistive terminations is excluded since it can be solved by using transformers.

Three examples of complex source impedances which are possible representations of external networks are presented. The case of load impedance can be similarly treated. A typical design of singly terminated filter is also described.

In describing the filter responses, the following abbreviations are used: RC - reflection coefficient, RL - return loss, TL - transducer loss and IL - insertion loss.

II. THE FILTER MODEL

All the examples presented are based on a 6-pole model, centered at 4000 MHz with 1% (40 MHz) bandwidth. The structure of the filter network is shown in Fig. 1. The nonzero elements of the coupling matrix **M**, as used for our examples, are illustrated in Fig. 2.

The solutions of the examples are given in terms of the nonzero couplings and transformer ratios. Since the coupling matrix **M** is symmetrical only the distinct coupling values are given, e.g., for $M_{12} = M_{21}$, only M_{12} is given. The terminations, as shown in Fig. 1, are normalized such that we have the load resistor $R_L = 1\ \Omega$ and the voltage source $E = 1$ V with an impedance Z_S which will be defined for each example.

III. DESIGN 1

Source Impedance

Constant (frequency independent) impedance $Z_S = 1 + j\,0.1$.

Solution

$$M_{12} = 0.88699$$

$$M_{23} = 0.51797$$

$$M_{34} = 0.85182$$

$$M_{45} = 0.51107$$

$$M_{56} = 0.86411$$

$$M_{16} = 0.11922$$

$$M_{25} = -0.38887$$

$$n_1^2 = 1.13168$$

$$n_2^2 = 1.10210$$

Simulated Responses

Lower stopband:		–	3976 MHz, minimum TL 30.6 dB
Passband:	3980	–	4020 MHz, minimum RL 20 dB
Upper stopband:	4024		MHz, minimum TL 31.6 dB

The simulated responses are also shown in Figures 3 and 4.

Starting Point*

$$M_{12} = M_{56} = 0.81777$$

$$M_{23} = M_{45} = 0.51110$$

$$M_{34} = 0.82430$$

$$M_{16} = 0.09330$$

$$M_{25} = -0.35710$$

$$n_1^2 = n_2^2 = 0.98239$$

* Source: Bandler and Chen [3].

Table of Subinterval Data

Frequency edges of subinterval (MHz)	No. of sample points	Step-length of extrema location	Specification	Weighting factor
3950 – 3970	4	2.0	RC = 0.9993	– 1.0
3970 – 3976	4	1.0	RC = 0.9993	– 1.0
3980 – 4020	13	0.5	RC = 0.1	1.0

Optimization Parameters

Variables: $M_{12}, M_{23}, M_{34}, M_{45}, M_{56}, M_{16}, M_{25}, n_1^2, n_2^2$

Initial step-length: 0.01

Accuracy requirement: 1.0×10^{-6}

Solution obtained after 48 iterations with 21 CPU sec.

IV. DESIGN 2

Source Impedance

$$Z_S = 1 + j\,0.15s, \quad s \triangleq \frac{\omega_0}{\Delta\omega}\left(\frac{\omega}{\omega_0} - \frac{\omega_0}{\omega}\right).$$

Solution

$$M_{12} = 0.8856$$

$$M_{23} = 0.5111$$

$M_{34} = 0.8243$

$M_{45} = 0.5111$

$M_{56} = 0.8178$

$M_{16} = 0.1010$

$M_{25} = -0.3571$

$n_1^2 = 1.15214$

$n_2^2 = 0.98239$

Simulated Responses

Lower stopband:		–	3976 MHz, minimum TL 34.2 dB
Passband:	3980	–	4020 MHz, minimum RL 20 dB
Upper stopband:	4024	–	MHz, minimum TL 34.2 dB

The simulated responses are also shown in Figures 5 and 6.

Starting Point

The same as the starting point of Design 1.

Table of Subinterval Data

Frequency edges of subinterval (MHz)	No. of sample points	Step-length of extrema location	Specification	Weighting factor
3950 – 3970	4	2.0	RC = 0.9993	–1.0
3970 – 3976	4	1.0	RC = 0.9993	–1.0
3980 – 4000	7	0.5	RC = 0.1	1.0

Optimization Parameters

Variables: $M_{12}, M_{23}, M_{34}, M_{45}, M_{56}, M_{16}, M_{25}, n_1^2, n_2^2$

Initial step-length: 0.005

Accuracy requirement: 1.0×10^{-6}

Solution obtained after 144 iterations with 42 CPU sec.

Comment

The starting point used here is actually a 6th order optimal design for resistive terminations, as has been described in [3]. Simulation shows that the responses of our solution for $Z_S = 1 + j0.15s$ are identical to the responses of the starting point with $Z_S = 1$. In other words, the optimum transmission characteristics have been recovered. We also notice that at the solution only two couplings, namely M_{12} and M_{16}, differ from their initial values. Both couplings are related to the first cavity.

In general, designing an optimal filter is equivalent to finding a one-port which has the desired input impedance. We denote Z_{in}^{o} as the input impedance of such a one-port that matches (w.r.t. certain specifications) a source impedance Z_S^{o}. Can we find a one-port with input impedance Z_{in} such that the same specifications can be satisfied for $Z_S = Z_S^{o} + j\alpha s$? The question is actually whether $Z_{in} = Z_{in}^{o} - j\alpha s$ can be realized by a one-port. In our case, it is not difficult to show that the input impedance of a singly terminated synchronously tuned multi-cavity filter has the following properties: (i) Re (Z_{in}) is an even function of s, (ii) Im (Z_{in}) is an odd function of s, (iii) the degree of the numerator of Z_{in} is greater than the degree of the denominator by 1 and (iv) both the numerator and the denominator are Hurwitz. Since Z_{in}^{o} is realizable, it satisfies these properties. The addition of the term $j\alpha s$ will not destroy properties (i)-(iii). Hence provided α is small enough so that (iv) is not violated, a solution of $Z_{in} = Z_{in}^{o} - j\alpha s$ is feasible.

V. DESIGN 3

Source Impedance

$$Z_S = 1.0 + jX, \quad X \triangleq \begin{cases} \dfrac{0.1}{0.5s - 1.0} & \text{for } s = \dfrac{\omega_0}{\Delta\omega}\left(\dfrac{\omega}{\omega_0} - \dfrac{\omega_0}{\omega}\right) \le \dfrac{4}{3} \\ -0.3 - 0.45\left(s - \dfrac{4}{3}\right)^* & \text{otherwise} \end{cases}$$

*Linearization at $s = 4/3$ to avoid singularity in definition.

Comment

The source reactance X is also plotted vs. frequency in Fig. 7.

The purpose of our introduction of complex source impedance is to represent the external network by an equivalent model. The reactance X defined here is a more realistic model for an adjacent channel filter in a multiplexer structure. Denote s' as the normalized frequency w.r.t. the center frequency of the adjacent channel. We have $s' \approx s + \delta$, where δ is determined by the separation of the center frequencies. Then we can express the input impedance of the adjacent channel filter by a rational function $Z_{in} = M/N$, where M and N are polynomials in s' and degree(M) = degree(N) + 1. Seen through an impedance inverter the impedance becomes N/M and it is substantially reactive outside the passband. For a sufficiently large s' we can write

$$\frac{N}{M} = \frac{b(s')^{n-1} + \ldots}{(s')^n + a(s')^{n-1} + \ldots} \approx \frac{b}{s' + a} \approx \frac{b}{s + (a + \delta)} .$$

Therefore, a reactance of the form $X = b/(s+c)$ is a very reasonable approximation if we assume ideal junctions and spacings.

Solution

$$M_{12} = 0.86800$$

$$M_{23} = 0.51986$$

$$M_{34} = 0.85285$$

$M_{45} = 0.51018$

$M_{56} = 0.87050$

$M_{16} = 0.11492$

$M_{25} = -0.39038$

$n_1^2 = 1.07707$

$n_2^2 = 1.11083$

Simulated Responses

Lower stopband:		–	3976 MHz, minimum TL 30 dB
Passband:	3980	–	4020 MHz, minimum RL 20 dB
Upper stopband:	4024	–	MHz, minimum TL 29 dB

The simulated responses are also shown in Figures 8 and 9.

Starting Point

The same as the starting point of Design 1.

Table of Subinterval Data

Frequency edges of subinterval (MHz)	No. of sample points	Step-length of extrema location	Specification	Weighting factor
3980 – 4020	9	0.5	RC = 0.1	1.0
4024 – 4030	4	1.0	RC = 0.9995	–10.0
4030 – 4050	4	2.0	RC = 0.9995	-10.0

Optimization Parameters

Variables: $M_{12}, M_{23}, M_{34}, M_{45}, M_{56}, M_{16}, M_{25}, n_1^2, n_2^2$

Initial step-length: 0.005

Accuracy requirement: 1.0×10^{-6}

Solution obtained after 27 iterations with 8.5 CPU sec.

Comment

Comparing Fig. 8 to Fig. 3, the resemblance between them is easily recognized. They are almost each other's mirror images w.r.t. the center frequency.

Take a first order Taylor expansion of

$$jX = j\,\frac{0.1}{0.5s - 1.0} \approx -j\,0.1 - j\,0.05s, \quad \text{for}\,|s| < 2.0.$$

Recall that in Design 1 we have defined $Z_S = 1.0 + j\,0.1$. Obviously, a $Z_S = 1.0 - j0.1$ would lead to a mirror image design. Also, from Design 2 we know that the term $-j0.05s$ can be compensated. This explains the above observation.

VI. DESIGN 4

Filter Type

Fully-elliptic function singly terminated filter. $Z_S = 0$.

Solution

$$M_{12} = 0.60371$$

$$M_{23} = 0.45292$$

$$M_{34} = 0.88167$$

$$M_{45} = 0.59971$$

$$M_{56} = 1.18094$$

$$M_{16} = 0.12783$$

$$M_{25} = -0.42475$$

$$n_1^2 = 1.78185$$

$$n_2^2 = 0.66598$$

Simulated Responses

Lower stopband:		–	3976 MHz, minimum IL 36.6 dB
Passband:	3980	–	4020 MHz, maximum IL 0.09 dB
Upper stopband:	4024	–	MHz, minimum IL 36.6 dB

The simulated responses are also shown in Figures 10, 11 and 12.

Starting Point*

$$M_{12} = 0.63086$$

$$M_{23} = 0.51092$$

$$M_{34} = 0.82353$$

$$M_{45} = 0.69549$$

$$M_{56} = 1.31016$$

$$M_{16} = 0.0$$

$$M_{25} = -0.26537$$

$$n_1^2 = 0.6882$$

$$n_2^2 = 2.04417$$

* The starting point is obtained from the pseudo-elliptic function filter given by M.H. Chen [5]. A similarity transformation has been performed to move the coupling M_{36} to M_{25}.

Table of Subinterval Data

Frequency edges of subinterval (MHz)	No. of sample points	Step-length of extrema location	Specification	Weighting factor
3950 – 3965	3	3.0	IL = 35 dB	–1.0
3966 – 3976	4	1.0	IL = 35 dB	–1.0
3980 – 4000	6	0.5	IL = 0.13 dB	40.0
3979 – 4000	5	1.0	IL = 0.0 dB	–100.0

Optimization Parameters

Variables: $M_{12}, M_{23}, M_{34}, M_{45}, M_{56}, M_{16}, M_{25}, n_1^2, n_2^2$

Initial step-length: 0.005

Accuracy requirement: 1.0×10^{-6}

Solution obtained after 242 iterations with 76 CPU sec.

CONCLUSION

For a channel filter embedded in a multiplexer, the external network can be represented by a Thevenin's equivalent which, under certain assumptions and to certain extent, may be reduced to a simple form. As some tentative models, three types of source reactances with different frequency dependency have been introduced. They include a constant reactance, a reactance linearly dependent on frequency and an approximation of a rational impedance function. Filter designs associated with these source impedances have been generated by a computer program using an efficient simulation approach and a powerful minimax method. Singly terminated filters have been commonly employed in multiplexers. A fully-elliptic function singly terminated filter has been presented as well. Interesting observations and their possible implications have been exploited and discussed.

Our examples have demonstrated that various network structures can be efficiently accommodated utilizing modern CAD techniques. It is hoped that upon a proper choice of network models, this advantage can be further exploited to provide a more efficient and practical approach to the design of channel filters and multiplexers. Such a prospect makes our work very attractive.

ACKNOWLEDGEMENT

The authors wish to thank S. Daijavad for the benefit of many fruitful discussions and suggestions.

REFERENCES

[1] J.W. Bandler and S.H. Chen, "Interactive optimization of multi-coupled cavity microwave filters", Department of Electrical and Computer Engineering, McMaster University, Hamilton, Canada, Report SOS-84-13-R, 1984.

[2] J.W. Bandler, S.H. Chen and S. Daijavad, "Efficient approaches to the simulation of narrow-band multi-cavity filters", Department of Electrical and Computer Engineering, McMaster University, Hamilton, Canada, Report SOS-84-9-R, 1984.

[3] J.W. Bandler and S.H. Chen, "Selected numerical examples of design optimization of multi-coupled cavity microwave filters", Department of Electrical and Computer Engineering, McMaster University, Hamilton, Canada, Report SOS-84-15-R, 1984.

[4] J.W. Bandler and S.H. Chen, "Case study of 10th order elliptic and quasi-elliptic self-equalized multi-cavity filters", Department of Electrical and Computer Engineering, McMaster University, Hamilton, Canada, Report SOS-84-20-R, 1984.

[5] M.H. Chen, "Singly terminated pseudo-elliptic function filter", COMSAT Technical Review, vol. 7, 1977, pp. 527-541.

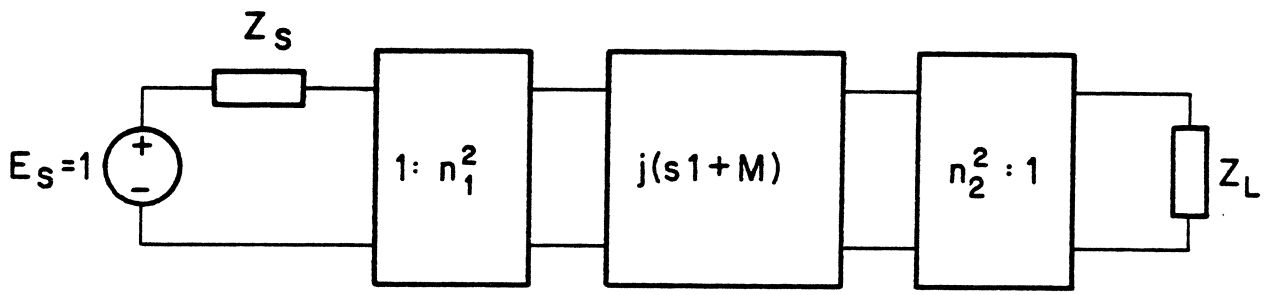

Fig. 1 Block representation of the overall network.

$$
\begin{bmatrix}
 & * & & & & * \\
* & & * & & * & \\
 & * & & * & & \\
 & & * & & * & \\
 & * & & * & & * \\
* & & & & * &
\end{bmatrix}
$$

Fig. 2 Nonzero elements of the coupling matrix

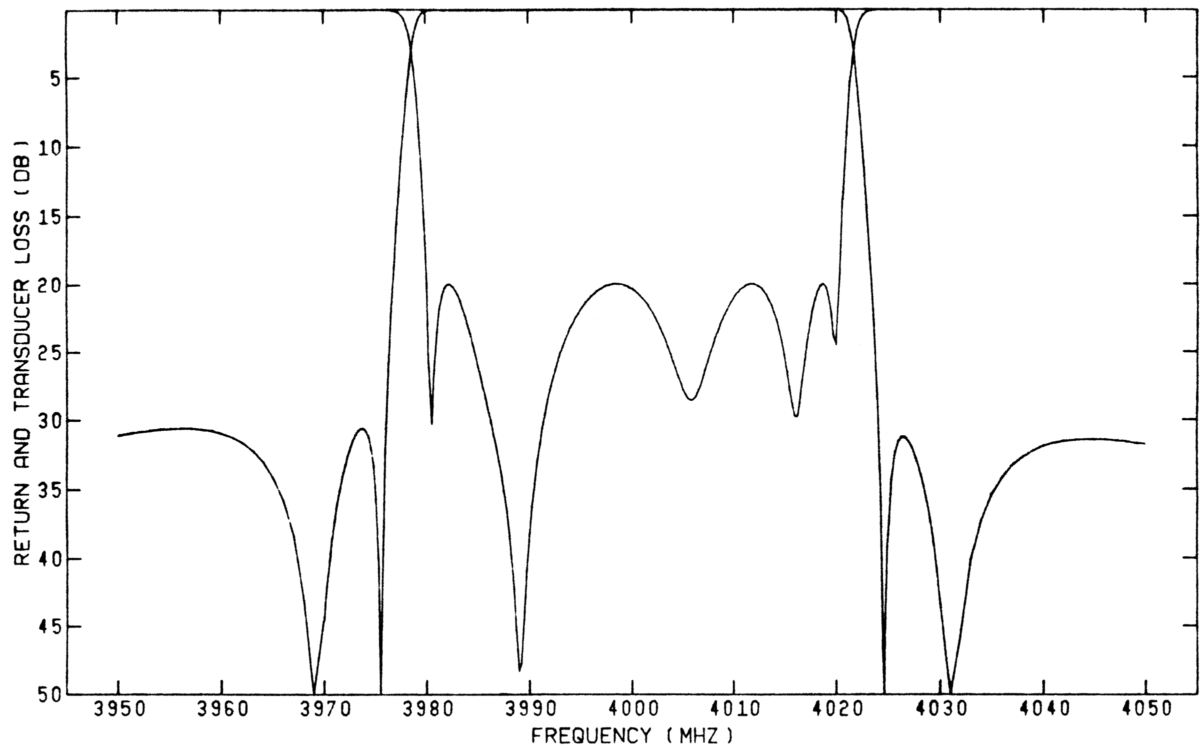

Fig. 3 Return and transducer loss of Design 1

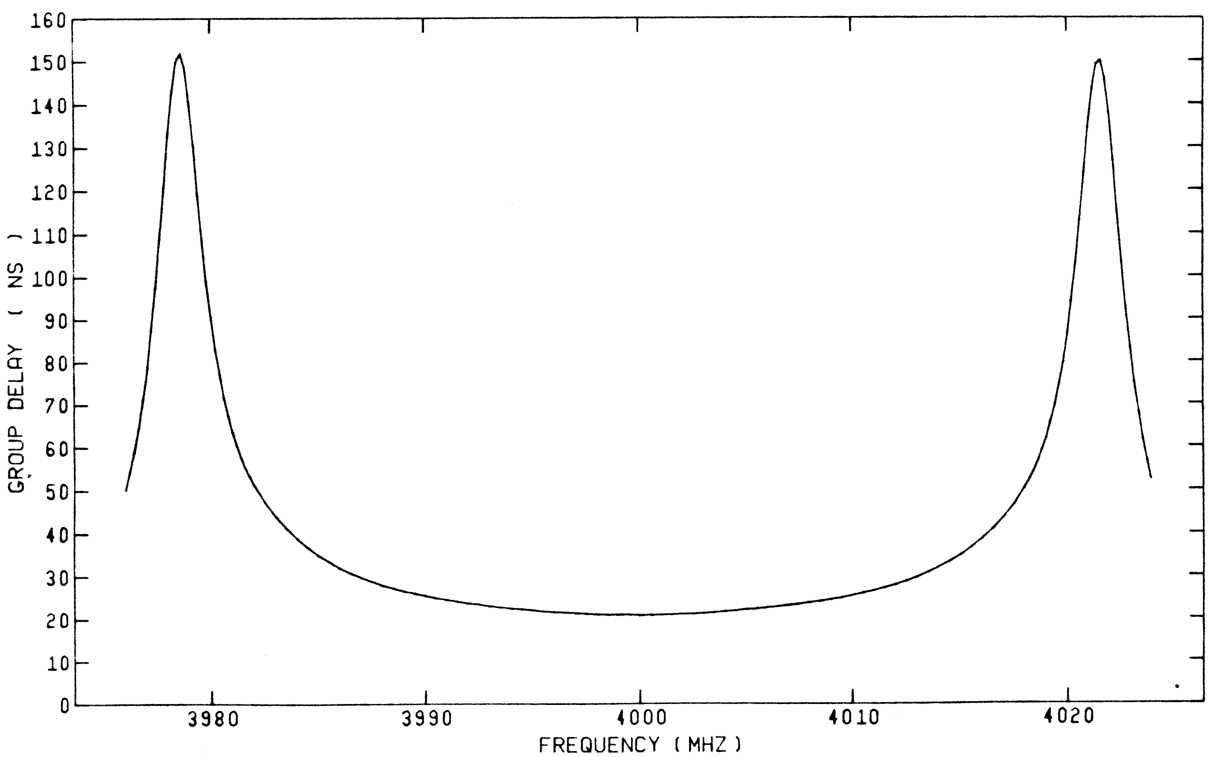

Fig. 4 Group delay response of Design 1

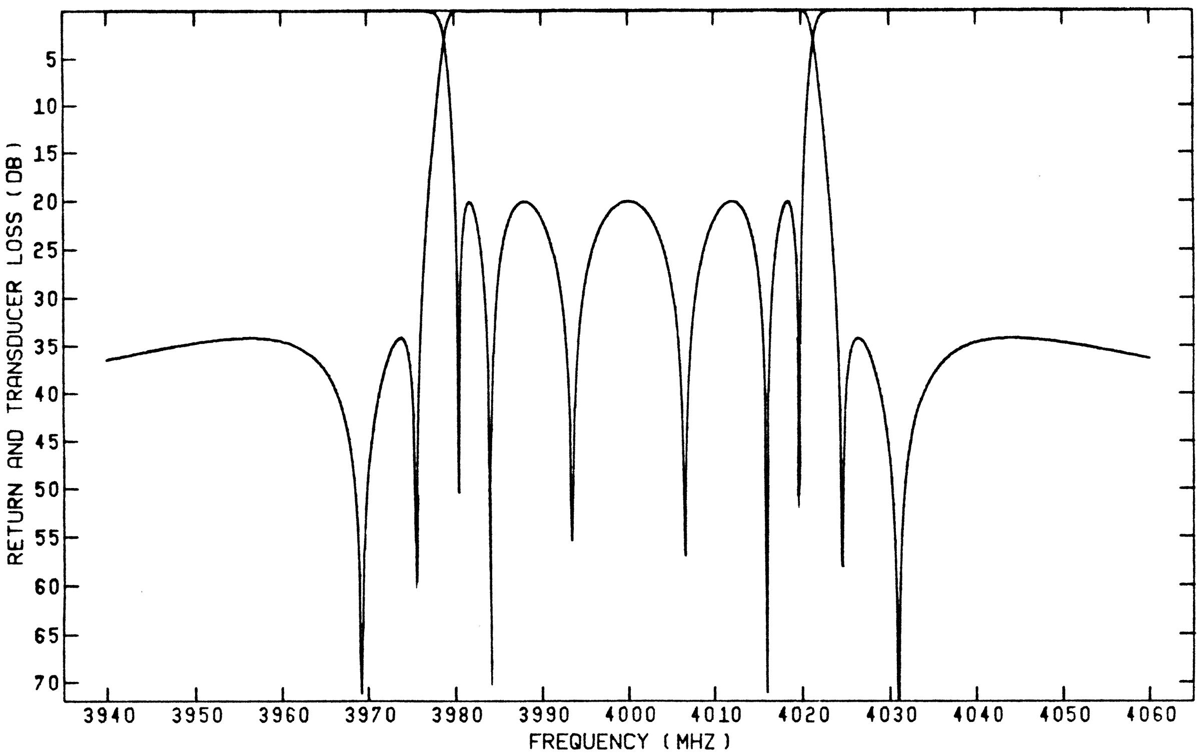

Fig. 5 Return and transducer loss of Design 2

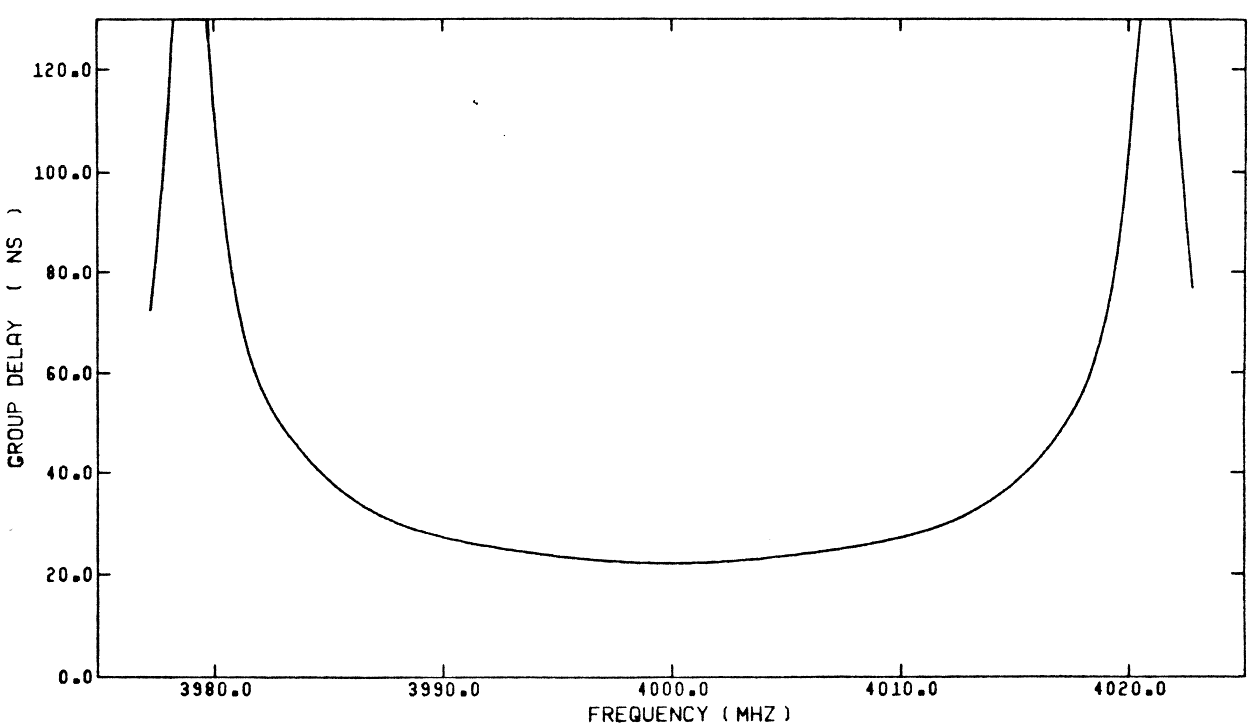

Fig. 6 Group delay response of Design 2

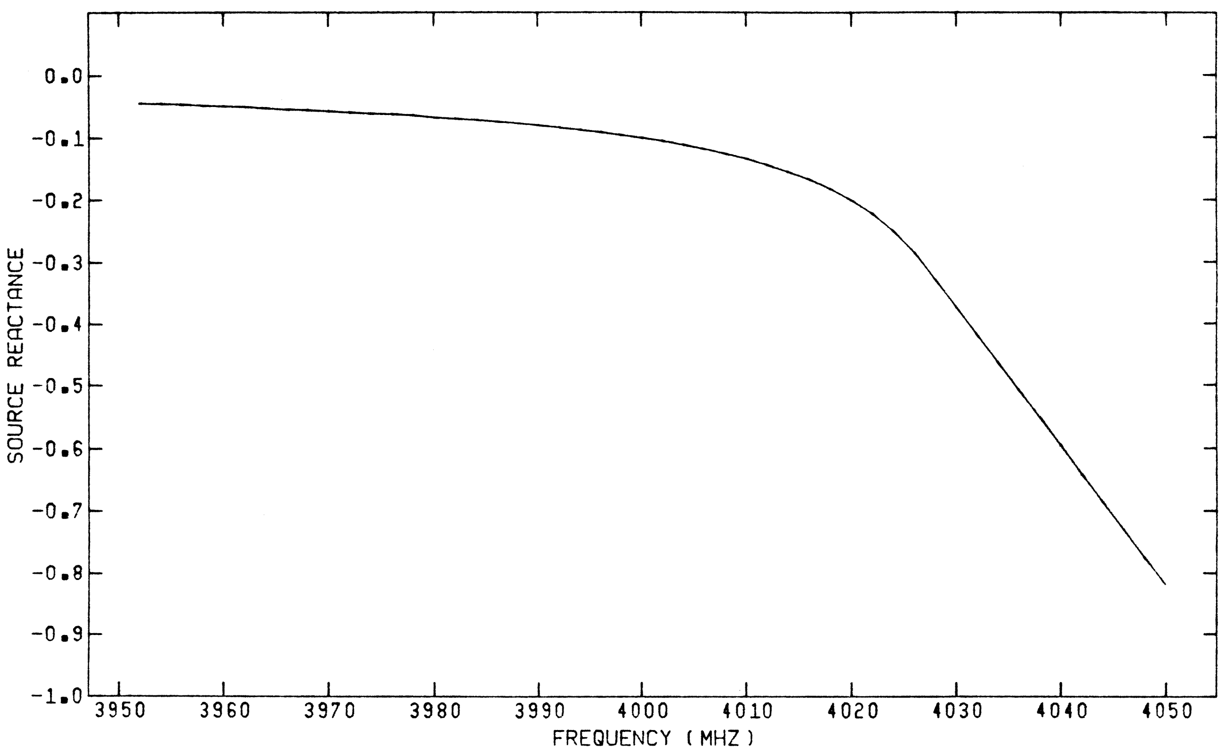

Fig. 7 The source reactance defined in Design 3

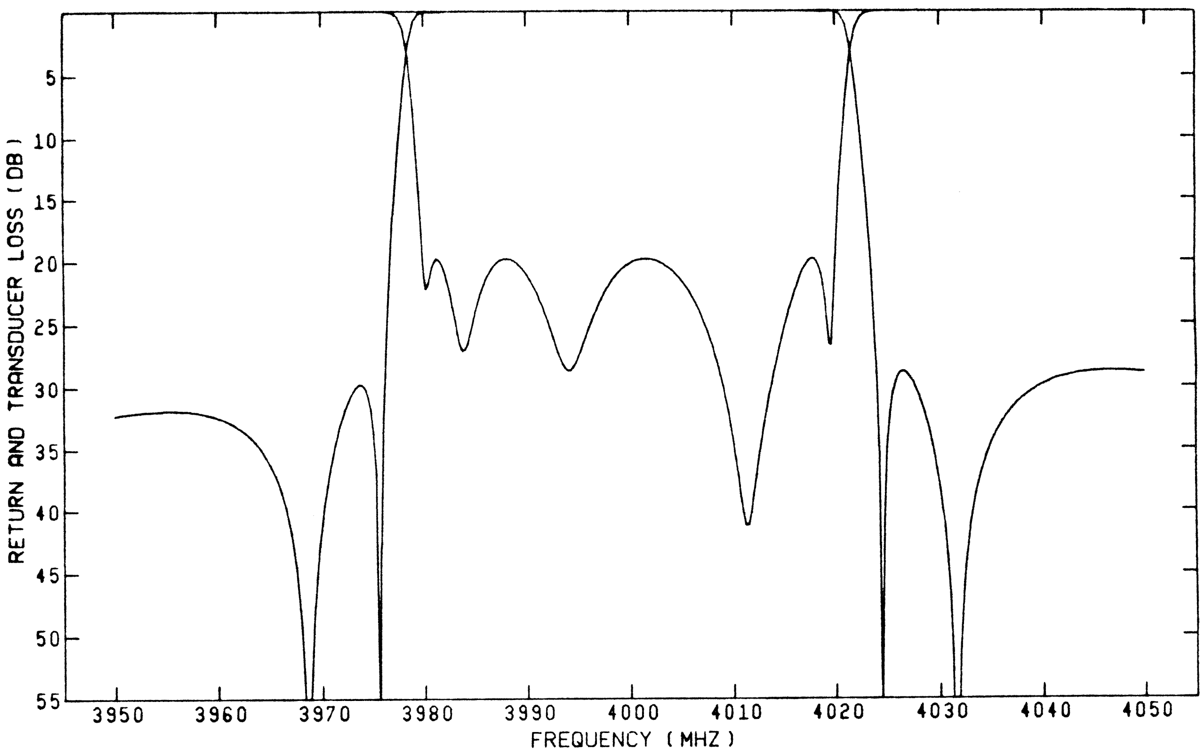

Fig. 8 Return and transducer loss of Design 3

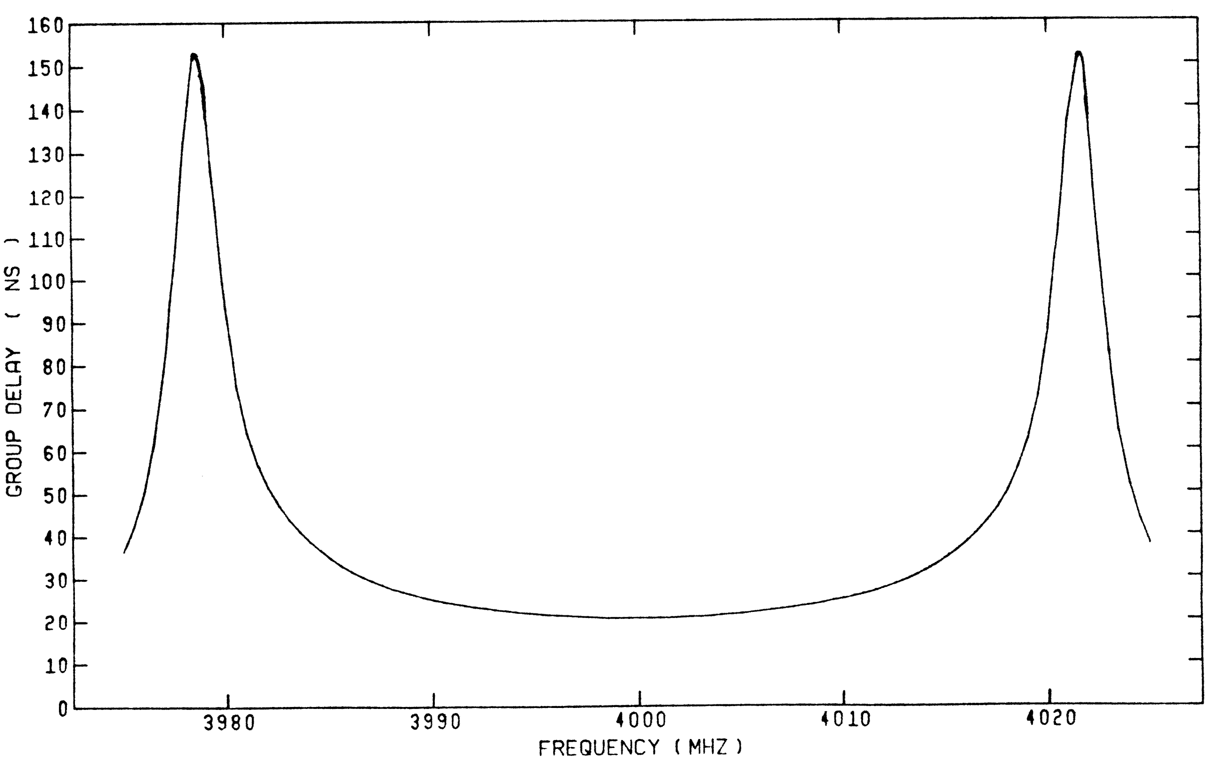

Fig. 9 Group delay response of Design 3

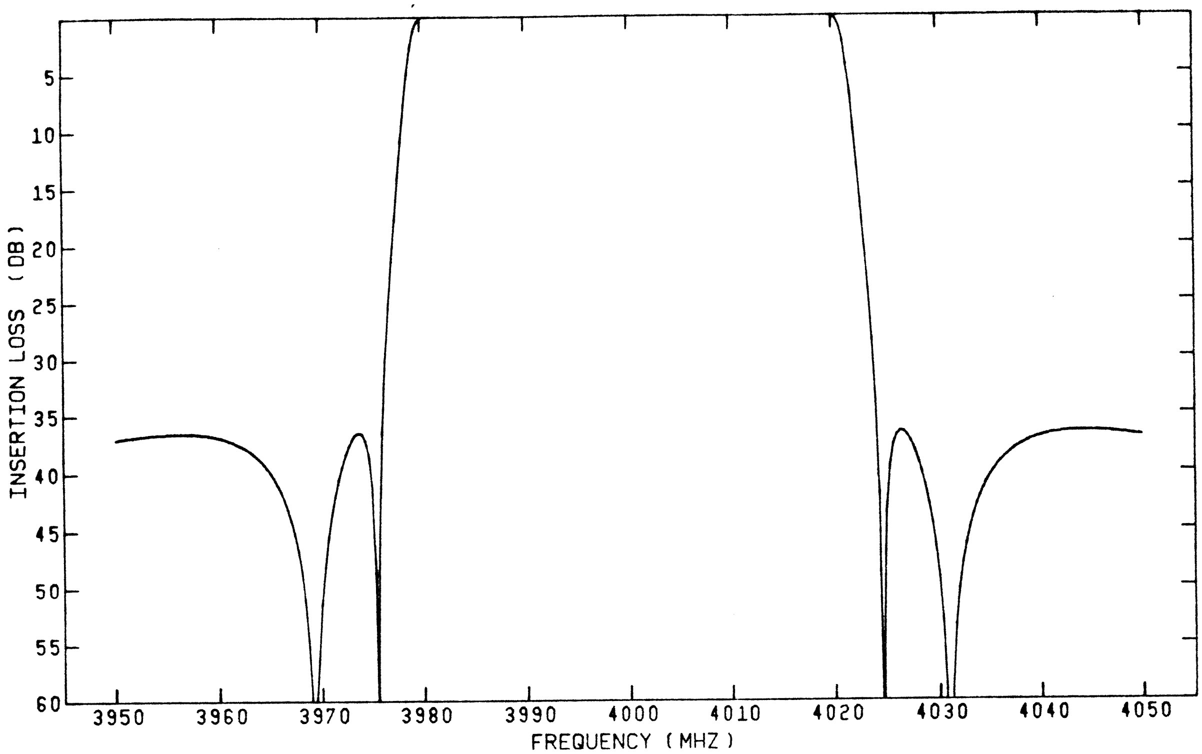

Fig. 10 Insertion loss of Design 4

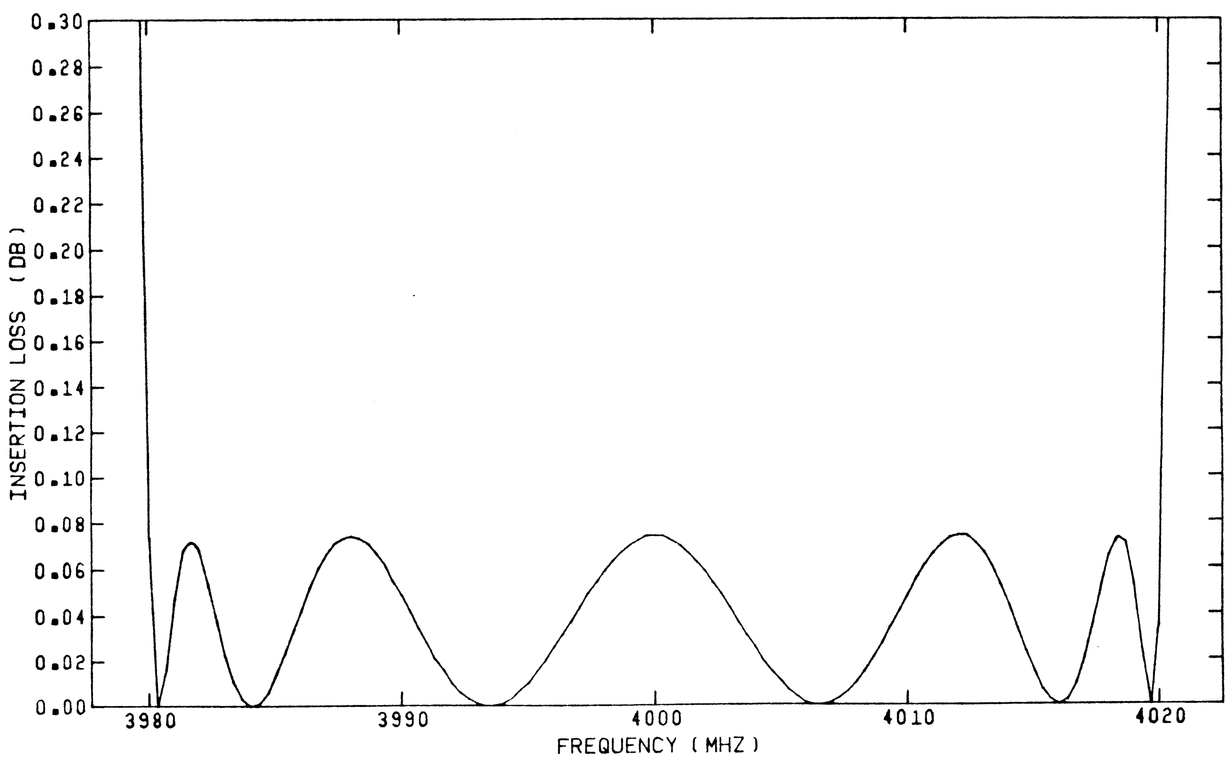

Fig. 11 Insertion loss for the passband of Design 4

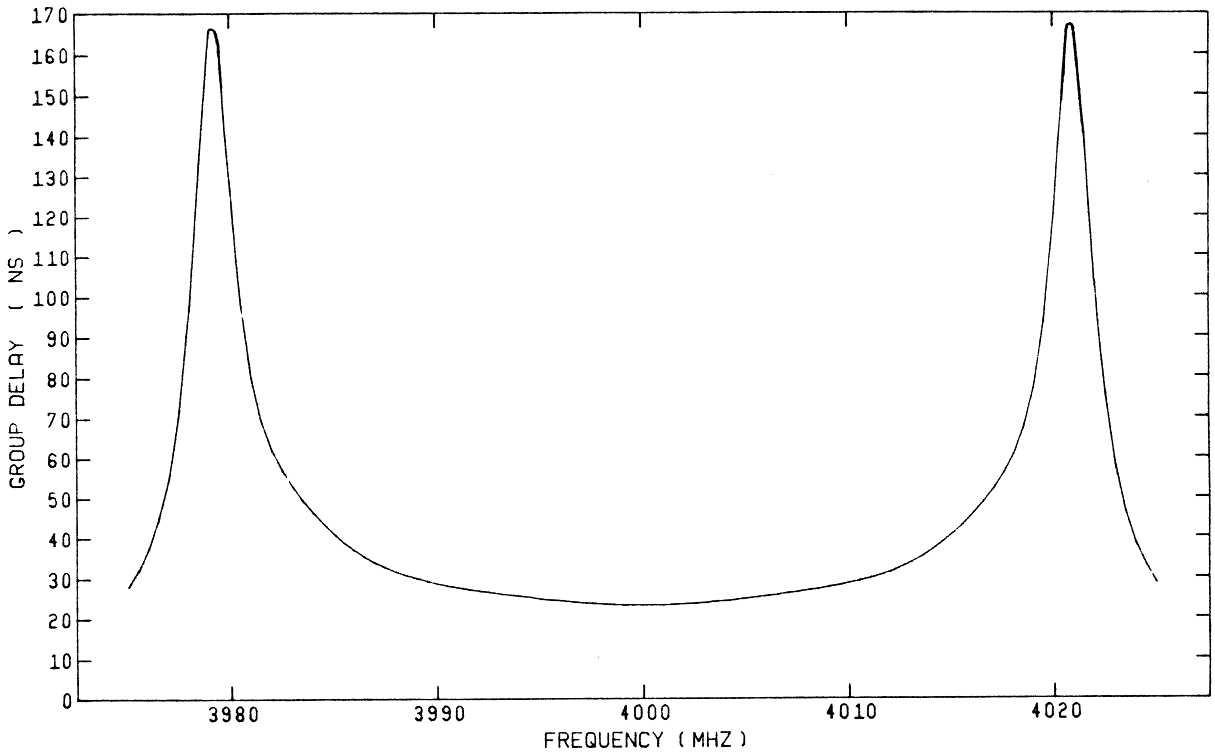

Fig. 12 Group delay response of Design 4